picoRing: battery-free rings for subtle thumb-to-index input

Ryo Takahashi
Meta Inc., Reality Labs Research
Redmond, Washington, USA
ryotakahashi@meta.com
takahashi@akg.t.u-tokyo.ac.jp

Eric Whitmire
Meta Inc., Reality Labs Research
Redmond, Washington, USA
ewhitmire@meta.com

Roger Boldu
Meta Inc., Reality Labs Research
Redmond, Washington, USA
rboldu@meta.com

Shiu Ng
Meta Inc., Reality Labs Research
Redmond, Washington, USA
shiung@meta.com

Wolf Kienzle
Meta Inc., Reality Labs Research
Redmond, Washington, USA
wkienzle@meta.com

Hrvoje Benko
Meta Inc., Reality Labs Research
Redmond, Washington, USA
benko@meta.com

Figure 1: Overview of picoRing. picoRing is a flexible sensing architecture enabling a variety of *battery-free* smart rings paired with a wristband. This paper shows four types of picoRing that support thumb-to-index finger pressing, sliding, or scrolling.

ABSTRACT

Smart rings for subtle, reliable finger input offer an attractive path for ubiquitous interaction with wearable computing platforms. However, compared to ordinary rings worn for cultural or fashion reasons, smart rings are much bulkier and less comfortable, largely due to the space required for a battery, which also limits the space available for sensors. This paper presents picoRing, a flexible sensing architecture that enables a variety of *battery-free* smart rings paired with a wristband. By inductively connecting a wristband-based sensitive reader coil with a ring-based fully-passive sensor coil, picoRing enables the wristband to stably detect the passive response from the ring via a weak inductive coupling. We demonstrate four different rings that support thumb-to-finger interactions like pressing, sliding, or scrolling. When users perform these interactions, the corresponding ring converts each input into a unique passive response through a network of passive switches. Combining the coil-based sensitive readout with the fully-passive ring design enables a tiny ring that weighs as little as 1.5 g and achieves a 13 cm stable readout despite finger bending, and proximity to metal.

CCS CONCEPTS

• **Human-centered computing → Interaction devices**.

KEYWORDS

coil, wearable, battery-free, ring, wristband, subtle finger input

1 INTRODUCTION

Hand and finger gestures are the primary ways to intuitively and seamlessly interact with wearable computing platforms, such as those provided by smart watches or smart glasses [28, 34, 40]. In particular, thumb-to-index finger microgestures support efficient and privacy-preserving inputs for wearable interaction [2, 4, 35]. Despite technical advances in wristband-based hand sensing [9, 38] and glasses-based computer vision [12, 13], high-fidelity detection and classification of the subtle and occluded thumb-to-index gestures including tap, pinch, and swipe remains challenging [16, 18, 38]. Some work has explored thumb-to-index finger inputs based on wristband sensing [38, 39], but they require relatively dynamic gestures for reliable classification or limit the input interface to either within-user, short-term usage for sufficient accuracy. By contrast, a ring-based device with physical inputs, like a button or slider, placed on the index finger offers a simple alternative with

unparalleled reliability for subtle thumb-to-index gestures [1, 14]. Such rings offer attractive and reliable interactive capabilities, but their form-factor is often bulky, largely due to the need to integrate a sufficiently sized battery.

In this work, we explore how two common device form-factors— a ring and wristband—can work together to unlock a new design space of small, battery-free rings for subtle thumb-to-index input. Because today's rings for micro finger gestures must power sensing and communication modules, their usability is hindered by the need for a bulky battery [18, 25, 26] or cumbersome power supply wiring [7, 21] in what would otherwise be a small, comfortable ring form factor. On the other hand, many users already wear a wristband all day long for health and fitness applications and for their convenient visual display, but typical hand interactions provided by a wristband requires dynamic, expressive hand gestures [16, 20, 41], which can be fatiguing or impractical in daily use. To fill this gap, we consider how a battery-free ring can complement a wristband by enabling a variety of reliable microgestures.

This paper introduces picoRing, a thumb-to-index finger input system enabling a battery-free, tiny, and lightweight ring-based input device (Figure 1). picoRing operates based on a pair of two coils: a ring-based fully-passive sensor coil and a wristband-based reader coil. Using a coil-based readout technique called passive inductive telemetry (PIT) [31, 32], the wristband coil wirelessly monitors the passive response of the ring coil caused by user inputs. First, the ring coil, which consists of a passive resonant coil connected to a physical switch, can passively convert the subtle thumb-to-index finger action (e.g., pressing the switch) into a unique passive response (i.e., the change of the ring's resonant frequency). Then, the wristband coil, which couples with the ring coil via a weak inductive field, can recognize the finger input by detecting the shift of the ring's resonant frequency. Because the ring operates by modifying the inductive field in a passive manner and does not require active signal transmission, the ring can be battery-free.

Unlike semi-passive readouts like near-field communication (NFC) and radio-frequency (RF) backscatter [22, 24], fully-passive PIT-based systems [31, 32] can eliminate the need for powering up the ring, enabling a chipless and simple ring design. Prior PIT-based input systems [31] leveraged passive input for detecting taps on surfaces. However, systems like TelemetRing [31], which requires a large (e.g., 9 cm-diameter) uncomfortable wristband coil to capture the ring's weak response, is not suitable for wearable usage and is primarily designed for simple taps. In contrast, picoRing stands out due to its versatility and practicality. Specifically, picoRing introduces four types of rings of mass 1.5 to 2.9 g for subtle thumb-to-index inputs including pressing, 1-D/2-D sliding, or scrolling with a network of different passive switches. Moreover, picoRing increases the PIT sensitivity by about ten times through a design optimization process at a higher frequency band from 13.5 MHz to 27 MHz. This results in a 5 cm-diameter-sized compact wristband coil demonstrating a stable readout distance of approximately 13 cm, regardless of finger bending or wrist in proximity with metallic items. Such a compact implementation of the wristband and ring increases the practicality of this approach and allows integration of picoRing into standard ring and wristband accessories.

Our contribution is summarized as follows:

- The practical design of a sensitive PIT technique to pair a battery-free ring coil with a compact wristband coil.
- The demonstration and technical evaluation of four types of rings, each below 3 g for subtle thumb-to-index input.

2 RELATED WORK

This section focuses on prior work which can recognize finger gestures by instrumenting an input system around the hand. For more detail on other prior work, please refer to [16, 18].

2.1 Instrumented hand

A wristband serves as a convenient location for detecting finger movements based on force measurement [9], EM wave [19], inertial sensing [20], capacitive coupling [28], electromyography (EMG) [30], computer vision [37], etc. Because the wristband infers finger gestures away from the wrist, the signal caused by subtle finger motions inevitably becomes small, challenging for the wristband to stably detect and accurately distinguish them [37, 38]. The use of machine/deep learning algorithm [19] and sensor fusion approach [38] can improve the recognition accuracy of the various finger gestures, and also recognize user-defined input as customized input with a few-shot learning [39]. However, 1) the approach is limited to within-user/short-term usage, requiring periodic calibration [19], 2) the wristband needs not subtle but relatively dynamic finger motions to accurately classify different gestures [39], or 3) the pure prediction accuracy significantly decreases when the wristband tries to recognize various subtle finger motions [38]. As a result, most wristband sensing rather focuses on the stable classification of expressive finger gestures [16, 20], possibly causing fatigue and discomfort for daily usage. In contrast, a finger-mounted device like a ring offers the advantages of close-range sensing for finger gestures, enabling reliable detection of subtle finger movements using a simple sensor and algorithm [7, 11, 17, 23, 25, 29]. Moreover, the sensing near the fingers can enable stable classification of micro, discrete finger gestures like tapping [18, 38], and mm-scale, continuous finger gestures such as sliding and scrolling [1, 7, 36], allowing imperceptible interactions in everyday life.

2.2 Ring-based input device

A ring positioned close to the index finger is an ideal accessory for implementing a thumb-to-index finger input system. Furthermore, the ring design that leaves the fingertip uncovered is more acceptable for daily use compared to other finger-mounted form factors like nails [5, 6]. Commercially, some smart rings (e.g., Oura Ring) are already available as healthcare monitoring. To detect subtle finger inputs, many standalone rings have been developed [10, 11, 17, 18, 25], but, prior rings are so bulky and heavy (> 10 g) due to the equipment of battery, signal processing circuit, and wireless communication module along with a sensor. Additionally, integrating these components into a small ring is complicated and costly. In contrast, the pair of a ring and a wristband enables a slimmer ring design by relocating the signal processing module from the ring to the wristband [26, 31]. For example, a ring equipped with a passive magnet [1] or an oscillating coil [26, 27], which can transmit a varying signal related to finger movement to a signal-processing

wristband, can be lightweight (< 5 g), compact, and tiny. Nevertheless, the ring itself remains bulky compared to the standard ring because it requires either a bulky magnet or a battery-driven oscillator to transmit the strong static or dynamic inductive signal to the wristband.

2.3 Battery-free ring-based sensor

To eliminate the battery from the ring connected to the wristband, RF backscatter [24], inductive power transfer [33], and PIT [31] are promising. RF backscatter operates a low-powered semi-passive antenna tag by harvesting environmental energy and reflecting an incoming RF signal from a reader antenna. Unfortunately, the EM interaction of the RF signal with the body can degrade communication performance, which requires a reader with W-class high input power. Moreover, the signal path is affected by unrelated hand movements, which could be misclassified as false positive. Inductive power transfer, which wirelessly transmits power to a ring-based coil via a wristband-based coil, also suffers from a low efficiency below 1% due to a large size ratio of the tiny ring and the compact wristband and relatively long distance between the ring and the wristband [31]. As a result, the input power from the wristband potentially exceeds 5 to 10 W considering 1% efficiency at best and over 100 mW power consumption of the communication module in the ring. Such high power levels are impractical for the power design of wristband devices.

In contrast, PIT based on an inductive link can reliably read out the sensor value from a fully-passive ring coil via a wristband coil without powering up the ring, as detailed in § 3.2. However, the prior PIT proposed by TelemetRing [31], which is most similar to picoRing's underlying technology, requires a 9 cm-diameter-sized large wristband coil due to its insufficient sensitivity. This is not suitable for wearable applications as it leaves a big gap (>3 cm) around the wrist. Unlike TelemetRing, picoRing offers distinct advantages including 1) the stable connection of the battery-free ring with a flexible 5 cm-diameter wrist-sized compact wristband, and 2) the sensing capability to detect various subtle finger movements using various battery-free rings.

3 THEORY OF OPERATION

3.1 System overview

picoRing consists of two main components: 1) a ring-based fully-passive sensor coil (i.e., ring coil) that passively changes its resonant frequency based on the user's thumb-to-index input to a passive switch such as a tactile or slider switch and 2) a wristband-based reader coil (i.e., wristband coil) that detects a peak in the frequency response corresponding to the resonant frequency of the ring coil (Figure 2a). The working principle is as follows (Figure 2b): First, the ring coil picks up the inductive field emitted by the wristband coil. Then, the ring coil causes a strong induced current in the wristband coil around the ring's resonant frequency based on Faraday's law of induction. Note that the resonant frequency of the ring is calculated as follows: $f_0 = 1/\left(2\pi\sqrt{L_{\text{sensor}}C_{\text{sensor}}}\right)$ where L_{sensor} and C_{sensor} are inductance and capacitance of the ring coil. The current also causes an impedance change in the wristband coil around f_0. Finally, a switch-based variable capacitor connected to the ring coil can convert the user's input such as press to the

shift of f_{sensor} by passively changing C_{sensor} via the on/off of the switch. Finally, a reader board connected to the wristband coil can recognize a tiny impedance change in the frequency response using a sensitive impedance measurement circuit and a sensitive peak detection algorithm, as will be explained in § 3.2 and § 3.3.

3.2 Sensitive passive inductive telemetry

picoRing needs to increase the sensitivity of prior PIT techniques [31] because the large size ratio and long distance between the ring and wristband weaken the passive response significantly. Basically, the passive response strengthens with the increase of the three factors: distance between wristband/ring coils (coupling coefficient: k), the inductance of the coils (L), and resonant frequency (f_0). When the wristband coil inductively couples with the ring coil as shown in Figure 2c, the input impedance of the wristband coil (Z_{load}) changes based on the passive response (ΔZ_{reader}) as follows:

$$Z_{\text{sensor}} = \begin{cases} R_{\text{sensor}} + j\left(\omega L_{\text{sensor}} - \dfrac{1}{\omega C_{\text{sensor}}}\right) & (f \neq f_0) \\ R_{\text{sensor}} & (f = f_0) \end{cases} \quad (1)$$

$$Z_{\text{load}} = Z_{\text{reader}} + \frac{(\omega M)^2}{Z_{\text{sensor}}} \quad (2)$$

$$= Z_{\text{reader}} + \Delta Z_{\text{reader}} \quad (3)$$

where $\omega\ (= 2\pi f)$ is an angular frequency, $M\ (= k\sqrt{L_{\text{reader}}L_{\text{sensor}}})$ is mutual inductance between the wristband and ring coils, Z_{reader} and Z_{sensor} are impedance of the wristband and ring coils consisting of the coil loss (R), the coil inductance (L), and the chip capacitor for tuning a resonant frequency of the coil (C), respectively, and ΔZ_{reader} is the impedance change caused by the ring coil. ΔZ_{reader} has a large peak around f_0 because Z_{sensor} remains only a small real impedance R_{sensor} at f_0 cancelling a large imaginary impedance ωL_{sensor} by $1/(\omega C_{\text{sensor}})$. Thus, the wristband can estimate the resonant frequency of the ring by detecting the peak in Z_{load}. Unfortunately, the extremely weak k below 0.002 in picoRing makes ΔZ_{reader} below 1 mΩ, which makes it hard for the wristband to capture such a small peak.

To increase ΔZ_{reader} under the low k, one simple solution is to design wristband and ring coils with a high L or high f_0. However, the short wavelength at a high f_0 prevents increasing the turn number of the coil. Thus, prior PIT uses either a high L (>10 μH) at a low f_0 (kHz) or a low L (<1 μH) at a high f_0 (tens of MHz), which inevitably results in small ΔZ_{reader} under the low k. To solve this trade-off, picoRing employs distributed capacitance arrangement (DCA) technique, enabling a high L at a high f_0 [8]. DCA separates a long coil into multiple shorter coils by inserting multiple chip capacitors in series. With this configuration, each short coil can behave as a small L (Figure 2c). Because the multiple small L are connected in series, the coil with a large turn number comprised of a long wire can behave as a high L (μH) at the high f_0 (MHz), which can increase ΔZ_{reader} under the low k.

Although DCA strengthen the passive response, it is still relatively weak ($\Delta Z_{\text{reader}} \approx 50$ mΩ) because of the low k (~ 0.001). To detect such a small impedance change, picoRing then employed a balanced bridge circuit [31]. Unlike a standard impedance measurement circuit which measures the target impedance itself, the
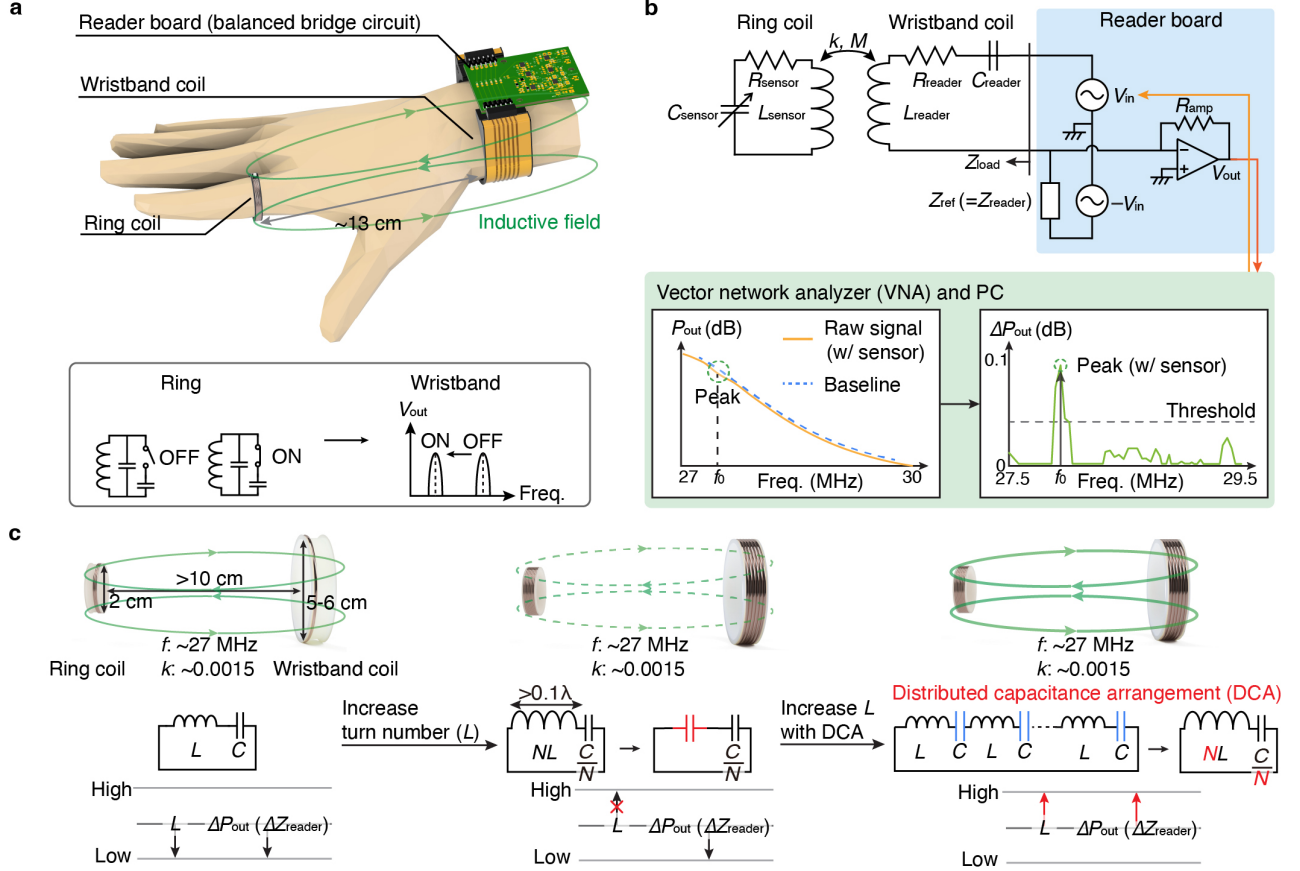
Figure 2: picoRing design. (a) The system illustration of picoRing. picoRing is based on passive inductive telemetry (PIT), in which the wristband coil wirelessly monitors the passive response of the ring coil caused by user inputs. (b) The circuit diagram and signal processing of picoRing which consists of a ring-based fully-passive sensor coil and a wristband-based reader coil connected to a reader board. (c) Overview of distributed capacitance arrangement (DCA) technique which can increase the passive response by enabling a high inductor at a high frequency.

bridge circuit can measure only the impedance change by using a differential structure (Figure 2c). Thus, the bridge circuit is useful for accurately measuring a small impedance change in an otherwise high impedance like with a thermistor or strain gauge. Here, picoRing uses the bridge circuit simply by matching a reference load (Z_{ref}) composed of chip elements with the wristband coil (*i.e.*, $Z_{reader} = Z_{ref}$). With this, the voltage output of the bridge circuit V_{out} can be calculated as follows with Eqn. 3, $Z_{ref} = Z_{reader}$, and $Z_{reader} \gg \Delta Z_{reader}$:

$$V_{out} = -R_{amp} \left(\frac{V_{in}}{Z_{load}} - \frac{V_{in}}{Z_{ref}} \right) \qquad (4)$$

$$\approx \begin{cases} R_{amp} \dfrac{\Delta Z_{reader}}{Z_{ref}^2} V_{in} \text{ (w/ ring coil)} \\ 0 \text{ (w/o ring coil i.e., } \Delta Z_{reader} = 0) \end{cases} \qquad (5)$$

where V_{in} is the input voltage of the bridge circuit, R_{amp} is the amplifier factor. Note that the real part of Z_{reader} is adjusted over $50\,\Omega$ with a chip resistor to meet the relationship of $Z_{reader} \gg$

ΔZ_{reader}. Eqn. 5 indicates that V_{out} is sensitive to ΔZ_{reader} by the matching process. Thus, the small peak (ΔV_{out}) appears in V_{out} via the bridge circuit (Figure 2c).

3.3 Resonance detection

Finally, picoRing needs to stably recognize the small peak (ΔV_{out}) in V_{out} despite the variations of V_{out} owing to the capacitive coupling with the body, the eddy current caused by the metal, EM noise from electric appliances, etc. To solve these challenges, picoRing uses a sensitive peak detection algorithm, which can find the peak through the error caused by a least-squared fitting of the frequency response (Figure 2c). First, the least-squared fitting function (*e.g.*, *scipy.polyfit*) estimates a smooth baseline from the raw magnitude output ($P_{out} = 20 \log_{10} V_{out}$) from the bridge circuit. Notably, the baseline is almost similar to the average line of P_{out}, which removes a small peak (ΔP_{out}) and noises in P_{out}. Then, the fitting error containing ΔP_{out} is derived by calculating the difference between the baseline and the P_{out}. Finally, a standard peak detection algorithm (*e.g.*, *scipy.find_peaks*) can find a clear peak against the
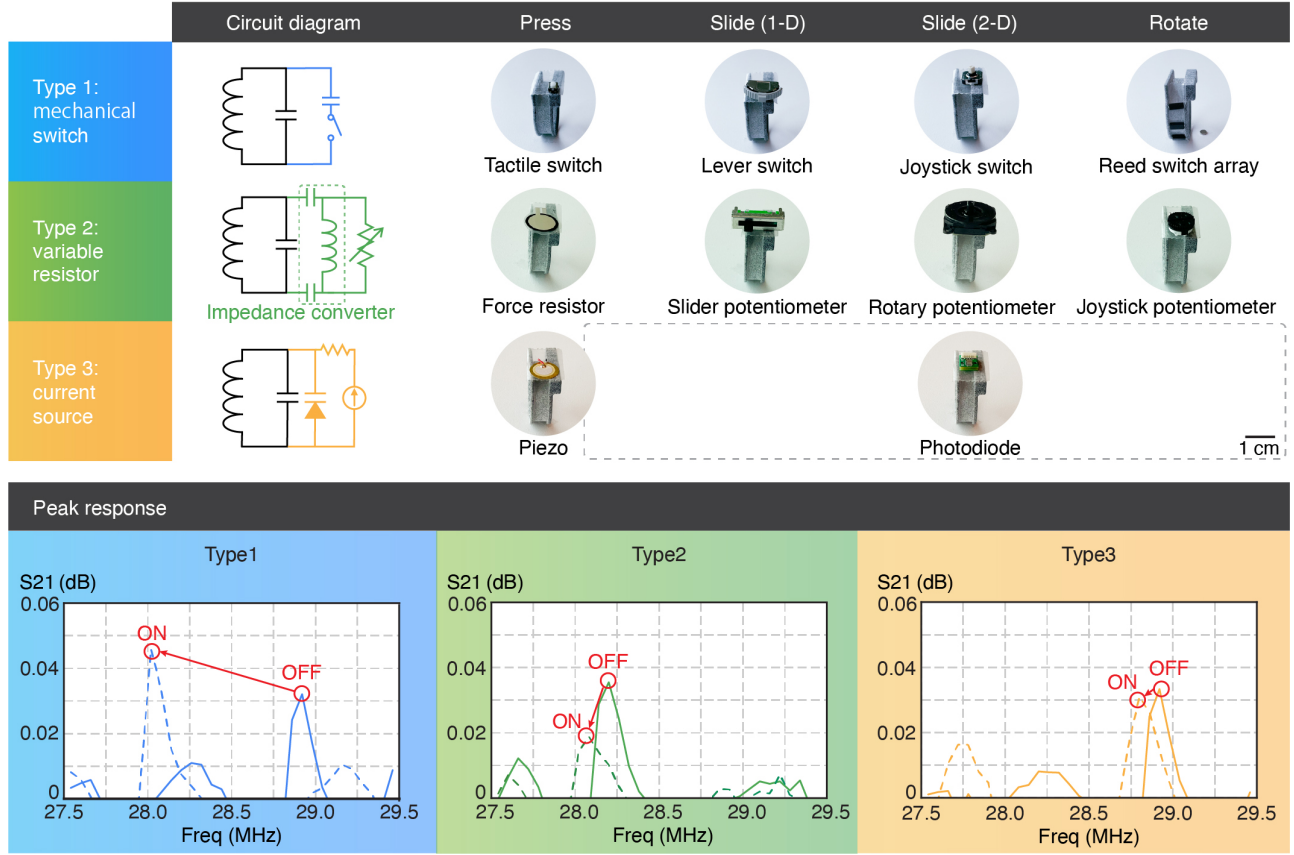
Figure 3: Design of passive variable capacitor. Among three types, picoRing uses type 1.

small noise (Figure 2c). The peak threshold was set to 0.02 dB, considering the dB RMS of a vector network analyzer (VNA) (0.002 dB), which converts V_{out} into P_{out}. Because the baseline is updated in real-time, the peak detection can be robust against the amplitude and frequency drift of V_{out}.

Unlike the prior PIT using DCA around 13.5 MHz frequency band [31], we note that picoRing uses DCA around the two times higher frequency band around 27 MHz to further increase prior PIT sensitivity, in addition to the unique peak detection algorithm. As a result, picoRing achieves sensitive readout of the fully-passive ring coil via the weakly-coupled compact wristband coil. Mathematically, the most critical technique to increase the SNR, or P_{out} is the distributed capacitance technique. The distributed capacitor increases the P_{out} by approximately 39 dB, while the bridge increases the P_{out} by approximately 19 to 25 dB at 29 MHz. The peak detection does not increase P_{out}, but it can detect a small peak. We experimentally checked that our peak detection can stably detect a small peak over 0.1 dB against the output drift (see § 6.5), resulting in the about 10x higher SNR.

4 DESIGN OF BATTERY-FREE RING COIL

In the context of AR/VR and human-computer interactions, subtle thumb-to-index finger inputs are frequently used as always-available and easy-to-use wearable controllers [16]. For example,

press, slide, and scroll finger inputs can complement touch or voice controls within the existing wearable devices to quickly access features, make selections, or control displays. Thus, this section explores how to recognize the press, slide, or scroll finger inputs via the ring coil. Because the wristband coil estimates the sensor state of the ring coil through the shift of the ring's resonant frequency ($f_0 = 1/(2\pi\sqrt{L_{\text{sensor}}C_{\text{sensor}}})$), picoRing focuses on how to design a passive variable capacitor reacting to the above finger inputs (Figure 3). One could also create a variable inductor, but this is more complicated, so in this work we limited our design space to variable capacitors.

There are three types of passive variable capacitors: type 1 based on a mechanical switch, type 2 based on a set of a variable resistor and an impedance converter circuit, and type 3 based on a set of a varactor and a passive current source (piezo or photodiode). Among the three types, picoRing needs a small and passive variable capacitor to embed the capacitor in the tiny and battery-free ring. Type 1 has low-cost and size advantages in addition to requiring users to only connect a tiny chip capacitor to the switch. As for type 2, the commercially-available variable resistor like the potentiometer is too bulky for a ring. Similar to type 2, type 3 requires a bulky battery because the passive current from the piezo or photodiode is too weak without a signal amplifier. Moreover, the frequency shift of type 2 and type 3 is much smaller

than the one of type 1. Thus, picoRing adopts type 1 sensors to a ring coil, as described in § 5.2. Specifically, picoRing uses a tactile switch, lever switch, or joystick reacting to press or 1-D/2-D slide input, respectively. Furthermore, picoRing uses the combination of the multiple reed switches and magnets to detect the scroll of the ring. Note that the use of the multi-functional switch could combine the above four switches together, but, currently-available multi-functional switch (*e.g.*, EVQWJN005, Panasonic) needs battery-driven active sensors near the switch to distinguish the direction of sliding or scrolling. Thus, this paper uses different passive mechanical switches for detecting pressing, sliding, or scrolling interactions.

5 IMPLEMENTATION

The following sections describe the implementation of both the wristband reader and ring-based sensor coil.

5.1 Wristband-based reader coil

The wristband coil consists of 1) a resonant coil implemented by flexible PCBs, 2) a flexible wristband implemented by 3D printing of elastomeric polyurethane, and 3) a readout board containing two magnetic connectors, the balanced bridge circuit connected to the external laptop-sized VNA (PicoVNA 106, Pico Technologies) and a laptop (Figure 4). To construct a proof-of-concept prototype, we selected the bulky PicoVNA for fast signal emission and acquisition, but, a set of a tiny VNA chip (ADL5960, Analog Devices) and a tiny FPGA (ICE40LP8K, Lattice Semiconductor) could be useful to implement a compact, low-powered, self-contained readout board. The turn number, size, and thickness of the coil are 6, 4.7×6.0 cm, and 2 mm, respectively. In addition, the resonant frequency, inductance, and resistance of the coil are 27 MHz, 3.7 μH, and 55 Ω, respectively. Using DCA, the coil was tuned by soldering eighteen 170 pF chip capacitors and one 51 Ω chip resistor in series. The coil with the larger turn number can further increase ΔZ_{reader}, but, accurate impedance matching with the chip elements becomes harder. Thus, the turn number of the coil was set to 6.

The coil was snapped on the readout board via magnetic spring connectors (Magnetic Connector 6 Contact Pins, Adafruit Industries). The bridge circuit follow a similar implementation to [31] and was implemented by multiple amplifiers available for a wide frequency band (LTC6228, Analog Device) and connected to a 5 V portable charger (Portable Charger, Anker). In total, the bridge consumed 430 mW (= 5 V × 86 mA). Note that the power consumption could be significantly lowered (≈ 20 mW) by simply replacing the current amplifier with the low-powered amplifier (e.g., LTC6253, Analog Device Inc.). R_{amp} was set to 100 Ω considering the gain product of the amplifier. The reference load was implemented by the chip elements. The impedance error between the reference load (Z_{ref}) and the coil (Z_{reader}) was approximately 5 to 10%, which was sensitive enough to recognize the small ΔZ_{reader}. With this setup, the VNA connected to the bridge circuit inputs a sweep signal to the bridge circuit ranging from 27 MHz to 30 MHz in steps of 60 kHz with a bandwidth of 10 kHz and an input power of 1 mW. Then, the VNA acquires the frequency response from the bridge circuit at approximately 5 fps and the laptop analyzes the response to detect the resonant frequency of the ring coil. Note the input
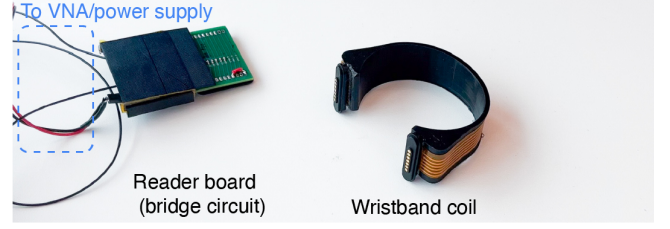

Figure 4: Implementation of a wristband coil.

Table 1: Physical specification of picoRing prototypes.

Ring	Weight	Width	Thickness
picoRing *press*	1.5 g	4.2 mm	1.5 mm
picoRing *slide*	2.9 g	5.6 mm	1.5 mm
picoRing *joystick*	2.7 g	5.6 mm	1.5 mm
picoRing *scroll*	2.5 g	8.8 mm	3.2 mm

power itself is a less crucial parameter since picoRing is required to measure the coupled ring's impedance through the power ratio of the input power and the output power in the wristband coil. For instance, even when we increased the input power above 1 mW, the SNR of the picoRing remained almost unchanged.

5.2 Ring-based sensor coil

The ring consists of a coil comprised of 24 AWG copper wire, a ring base, and a rigid sensor board. The turn number and size of the ring coil are 7 to 8, 1.9 cm diameter with the width of 4 to 9 mm. Note that the turn number was determined based on § 6.1 evaluation. Moreover, our preliminary investigations revealed that ISM frequency band above 40 MHz leads to inevitable electromagnetic interactions and increased impedance in the ring coil when worn on the hand, resulting in an SNR decrease. Specifically, we found that ring coils resonating at 13.56 MHz or 27.12 MHz exhibit minimal impedance change (5-10%), whereas coils tuned to 40.68 MHz experience significant impedance changes (over 50%) when worn. Consequently, we selected the 27.12 MHz band as the ring's resonant frequency. The ring base was SLS-printed with Nylon material. The sensor board was designed based on the circuit diagram of type1 (Figure 3), which consists of a pair of a mechanical switch and chip capacitors. Four types of mechanical switches were employed to detect basic subtle one-handed inputs: a tactile switch for pressing input, a lever switch and a joystick switch for sliding input in 1-D and 2-D, and a set of reed switches for scrolling input. For more detail, please refer to § 7 and Table 1.

6 TECHNICAL EVALUATION

To characterize how the peak signal varies with the coil parameters, finger movements, or surrounding objects, this section evaluates the signal-to-noise ratio (SNR) of picoRing for various conditions. To decouple the readout board from the common ground, we inserted two RF transformers (T1-1-X65+, Mini Circuits). Because of the inductive coupling's resilience against the body, the SNR characteristics of picoRing shows minimal variations for similar

Table 2: SNR, L_{sensor}, R_{sensor}, and the capacitor number for the turn number of a sensor coil tuned around 29 MHz.

Turn number	3	4	5	6	7	8	9
SNR	6.2	8.6	11.6	13.5	17.0	18.2	17.5
L_{sensor} (μH)	0.34	0.56	0.85	1.2	1.4	1.8	2.1
R_{sensor} (Ω)	0.89	1.1	1.5	1.8	2.0	2.6	3.4
Capacitor number	1	2	2	2	3	3	3

hand sizes. Thus, we conducted the following evaluations for a single user (man, 20s).

6.1 SNR for turn number

First, we evaluated the SNR for the turn number of the ring coil to decide the proper turn number of the ring coil. The ring coil was tuned at 29 MHz, and the turn number ranged from 3 to 9 in the step of 1. The distance between the ring and the wristband was set to 13 cm. The SNR was calculated as follows using S21 100 outputs $\left(P_{out}\ (dB) = 20\log_{10} V_{out}\right)$ of the VNA:

$$ SNR = \frac{\text{mean}\left(P_{out\ w/\ sensor}\right) - \text{mean}\left(P_{out\ w/o\ sensor}\right)}{\text{std}\left(P_{out\ w/o\ sensor}\right)} $$

SNR for the turn number was described in Table 2. The result indicated that the higher turn number results in a higher SNR, although the SNR varies little above 7 turns. This is because the coil loss (R_{sensor}) owing to the long wire and proximity effect between the wires becomes non-negligible as the turn number increases. Therefore, this paper employed 7 or 8 as the turn number of the ring coil. Following the next sections, we measured the SNR of the ring coil with turn number of 8.

6.2 SNR for frequency

To check the acceptable resonant frequency of the ring, we then examined the SNR for resonant frequencies ranging from 20 MHz to 40 MHz in 1 MHz step (Figure 5a). The distance between the ring and the wristband was set to 13 cm. The result showed that the sensitive readout band (SNR > 10) was 24 to 31 MHz because the impedance matching of the bridge circuit was adjusted at the center of 27 MHz. Note that at SNR below 10, or ΔP_{out} below 0.02 dB, it was difficult to distinguish the noise's peak robustly, as detailed in § 7.4. Therefore, we reject false positives by setting the peak threshold to be 10x higher than the noise floor. Based on the result, we used 27.5 to 29.5 MHz, which is a large enough band to monitor the peak shift of various picoRings, as will be described in § 7.

6.3 SNR for distance

Next, we evaluated the SNR for the readout distance to confirm the available distance between the ring and wristband coils. Figure 5b illustrates the result of SNR. First, we measured the SNR with and without the hand and confirmed that the SNR curve was almost the same, which means the inductive coupling between the coils interacts little with the body. Then, we compared picoRing (with no hand) to two baselines: (i) a standard PIT coil without DCA or

a bridge circuit, and (ii) a PIT coil tuned at 13.5 MHz similar to TelemetRing [31].

In (i), the wristband coil was a 1-turn, 50 Ω coil, and the ring coil was a 3-turn resonant coil tuned at 29 MHz and the VNA measured S11 (impedance) of wristband coil directly without the bridge circuit. In (ii), the wristband coil was a 6-turn resonant coil tuned at 13.5 MHz and the ring coil was an 8-turn resonant coil tuned at 15 MHz. Because picoRing uses a two times higher frequency than (ii), the P_{out} can increase at least $12 P_{out} (\approx\ 20\log_{10} 2^2 V_{out})$ times compared to (ii). The result shows that picoRing using the higher resonant frequency around 27 MHz increases its SNR by approximately 13 compared to (i)(ii) and the available readout distance of picoRing (SNR $\geq$ 10) reaches up to 15 cm ($k \geq 0.001$) with no misalignment between the coils. Considering the SNR decrease owing to the finger angle (§ 6.4), the available readout distance of the current picoRing is 13 cm (x2.3 reader's diameter).

6.4 SNR for finger bending

Then, we examined the SNR for finger angle because the inductive coupling (k) decreases due to the coil misalignment. Figure 5c shows the time-series SNR spectrum and the average SNR against the five distinct finger angles ($-30°$, $0°$, $30°$, $50°$, or $70°$). The distance between the ring and the wristband was set to 13 cm, and the ring was tuned at 29 MHz. The result shows that picoRing can successfully capture the ring's peak at 29 MHz against up to $70°$ finger bending, which is sufficient for the daily hand movement.

6.5 SNR for proximity metal

Lastly, we measured the SNR against six kinds of metallic objects in the proximity of the hand because the eddy current or EM noise generated from metallic electrical appliances could inductively influence both the ring and wristband coil. Figure 5d shows the time-series SNR spectrum and average SNR for the six items including Qi wireless charger (Magsafe Charger, Apple) attached to a smartphone (iPhone 13 Pro Max, Apple), a set of an NFC reader (DLP-7970ABP, Texas Instruments) and an NFC tag (TIDM-RF430-TEMPSENSE, Texas Instruments), a laptop (MacBook Air M2, Apple), a microwave oven (NE-EH228, Panasonic), a hair dryer (KHD-9300, KOIZUMI), and a smart ring (SOXAI RING 1, SOXAI). Note that the SNR evaluation was conducted during operation of the appliances such as 15 W charging of the smartphone with the Qi charger, 200 mW charging and communication of the NFC tag with the NFC reader, 700 W heating of the rice with the oven, etc. The result indicates that picoRing successfully detects a sharp peak at 29 MHz except for the smart ring placed near the ring coil. This is mainly because 1) for the readout board, the passive response from the ring coil is much higher than EM noise, and 2) the peak detection algorithm is robust against the output drift caused by the eddy current, as explained in § 3.3. Unfortunately, the resonant frequency of the ring coil is shifted up when the metallic ring within 1 cm distance of the ring coil (e.g., the metallic ring is worn either index or middle fingers) constructs a strong inductive coupling with the ring coil. Future work could utilize such a peak shift up as the hint of metal detection near the ring.
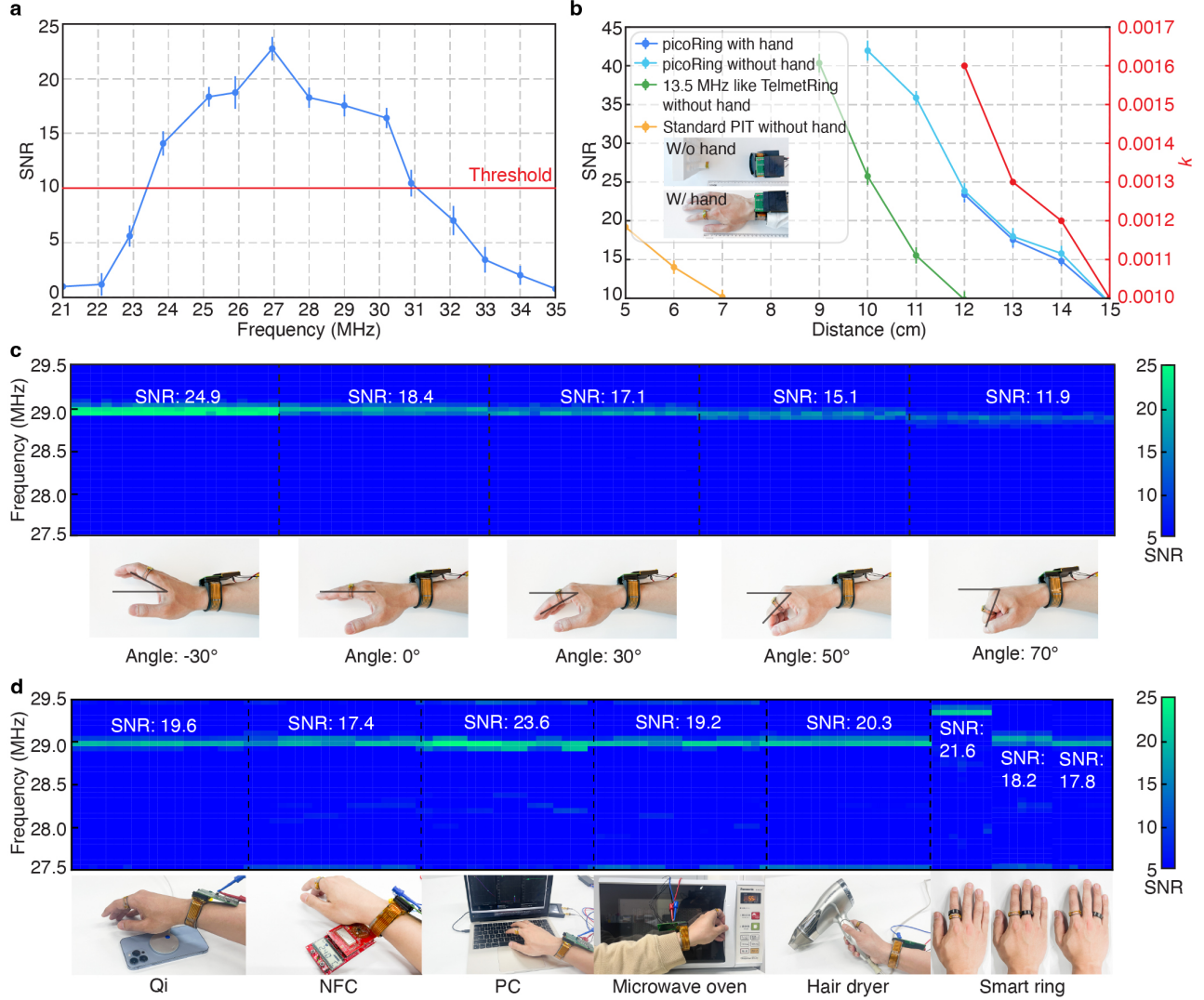
Figure 5: SNR evaluation of picoRing. (a) SNR for the resonant frequency of the ring coil. (b) SNR for the distance between the wristband and the ring. (c) SNR for different finger bending angles (d) SNR for proximity metallic items.

7 PICORING EXAMPLES

This section presents four examples of picoRing (Figure 6). Because of its easy-to-carry and always-available advantages, picoRing can potentially serve as a versatile input controller for ubiquitous devices, users, and situations. Although the current prototype is divided into four input structures and is less adaptive, future iterations could feature a more flexible and integrated design to accommodate a wider range of interactions, as detailed in § 8.

7.1 picoRing *press*

First, Figure 6a shows picoRing *press* for a music controller. picoRing *press* consists of 7-turn 2-layer resonant coil with a tiny tactile switch (EVQ-P2P02M, Panasonic), and the resonant frequency in *on/off* state was tuned at 28.9 and 28.0 MHz, respectively. Although

the thumb-to-index press action is the one of most fundamental inputs in wearable computing, the prior rings are bulky and heavy due to the battery equipment. Unlike them, picoRing *press* is tiny and lightweight (1.5 g) because picoRing can replace a bulky battery and a sensing/communication module with a lightweight fully-passive coil (Table 1). Thus, the battery-free, lightweight implementation of picoRing *press* can provide continuous, natural interactions without worrying about the battery management.

7.2 picoRing *slide* or *joystick*

Then, Figure 6b-c show picoRing *slide* designed for a movie controller and *joystick* for a game controller, respectively. picoRing *slide* that can detect center (idle), 2 mm or 4 mm left, 2 mm or 4 mm right slide, and press input, consists of a ring base and an 8-turn resonant coil with a lever switch (PLMG5-GH-V-T/R, Diptronics). The
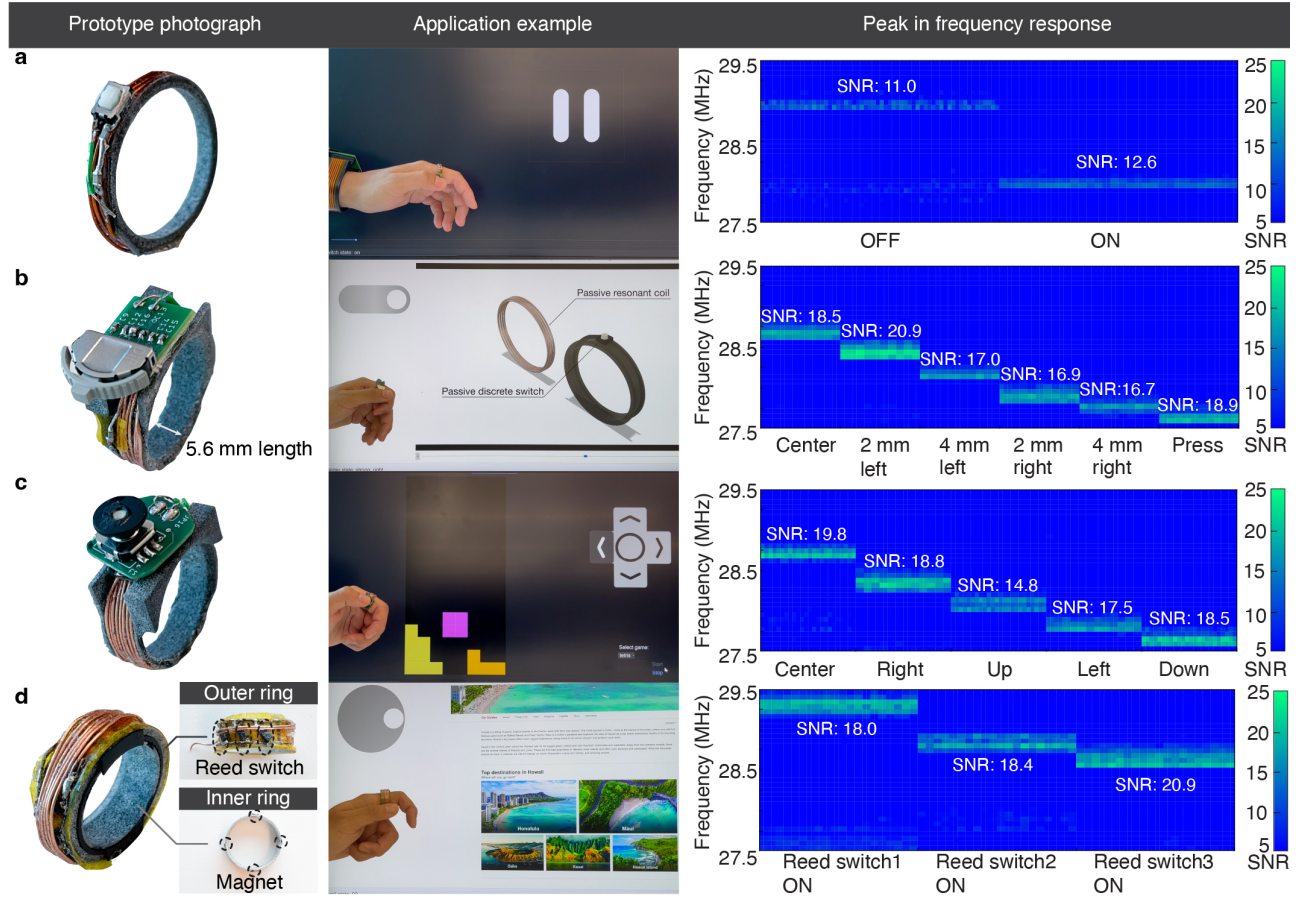
Figure 6: picoRing demonstration. Photograph, application example, and peak in the frequency response of picoRing (a) *press*, (b) *slide*, (c) *joystick*, and (d) *scroll*.

resonant frequency of five types of slide and press states was tuned at 28.7, 28.4, 28.1, 27.9, 27.7, and 27.6 MHz, respectively. Moreover, picoRing *joystick*, which can detect a center (idle), right, up, left, and down motion of the joystick, consists of a ring base, an 8-turn resonant coil with a joystick switch (SKRHAAE010, Alps Alpine), and a joystick knob. The resonant frequency of the five types of positions was tuned at 28.7, 28.4, 28.1, 27.8, and 27.6 MHz, respectively. The prior rings which needs user-dependent calibration for 1-D or 2-D subtle finger input [3, 17, 26]. However, picoRing, which directly senses the 1-D/2-D slide via the switch, can recognize the 1-D/2-D finger motions without any user-dependent calibration for each input, similar to standard physical-button-based video or game controllers. Such intuitive operation allows for easy and quick use of picoRing *slide* and picoRing *joystick* for various users and situations.

7.3 picoRing *scroll*

Next, Figure 6d shows picoRing *scroll* used as a page controller. picoRing *scroll* consists of an inner ring that has four tiny magnets with 2 mm diameter and 0.5 mm height, an outer ring that includes

an array of three reed switches (MK24-A-2, Standex-Meder Electronics), and a bearing ring with a 1.5 mm width between the inner and outer rings. Each part was 3D-printed using an SLS printer and Nylon material. The tiny magnet placed near the reed switch can activate the reed switch when the magnet is within 5 mm distance. This setup allows picoRing *scroll* to recognize the rotation of the outer ring with an approximate 45° resolution, considering the two states (*i.e*, on and off states) of three reed switches. The resonant frequency in *on* state of each reed switch was tuned at 29.3, 28.9, and 28.6 MHz. Note that picoRing *scroll* becomes relatively thick owing to the thickness of commercially-available tiny reed switch (see Table 1). However, picoRing *scroll* equipped with tiny magnets can radically reduce the risk of accidental contact with daily metallic objects, unlike the conventional ring-based scroll device equipped with bulky magnets [1]. As a result, the compact design of picoRing *scroll* can enhance its usability while ensuring seamless scrolling in various applications.

7.4 Input accuracy

Lastly, we invited three participants (one woman and two men) to evaluate how picoRing's input accuracy changes based on the

different users. Their hand size was almost similar to fit in the ring and wristband coils to their hand. First, we measured the SNR of picoRing *press*, *slide*, *joystick*, and *scroll* around 30 to 70° finger bending. Figure 6 shows the time-series SNR and the average SNR. The result shows that the average SNR of the four types of picoRing can be over the threshold of 10 dB. Then, we attached picoRing *press* to the users and measured the press recognition accuracy for the measured SNR ranging from 10 to 13. Here, we measured the recognition ratio of only picoRing *press* because picoRing *press*, which consists of the 7-turn coil unlike the 8-turn other picoRing, shows the smallest SNR. We observed that the recognition accuracy for the pressing of 300 (= 100×3 users) times was 99.7% around the SNR of $11 - 13$, but the recognition accuracy started degrading to 93.3% at the SNR of around 10. Such accuracy drop at the SNR of 10 is considered negligible since the users had to bend their wrist tightly, making it hard to input to the ring. While a more through evaluation dedicated for each input through Fitts's law is necessary, current picoRing shows technically sufficient high SNR, ensuring reliable recognition for pressing, sliding, and scrolling actions.

8 DISCUSSION

There are some limitations in the current picoRing. First, the current prototype needs four types of picoRing covering various thumb-to-index inputs. Although wearing four types of picoRing might be one of the solutions, the inductive interference between the ring coils, which has the almost similar resonant frequencies, inevitably causes wrong classification of finger inputs. Additionally, wearing multiple rings on a single index finger could compromise comfort and wearability. To solve this challenge, we would try to develop a tiny all-in-one switch supporting press, slide, and scroll interactions, as described in § 4, and also assign the different resonant frequencies to each interaction. Then, picoRing requires users to attach the two types of wearable devices—ring and wristband—unlike the prior single wearables like smartwatches. Next, our wristband device including the VNA function can potentially be miniaturized to the smartwatch size, although the current wristband requires the large VNA equipment, by referring to the S21 measurement circuit part (2 cm x 3 cm) of NanoVNA (open-source compact VNA).

Finally, the current prototype is designed for middle-sized hands. To be available for various hand sizes, we should quantitatively explore how the coil size, the distance, and the readout frequency affect the SNR. we also plan to examine subjective usability using System Usability Scale and NASA Task Load Index.

As for the future works, picoRing could be used to track the continuous finger movements utilizing the strength change of the inductive coupling according to the finger bending [15, 26]. Also, picoRing system could support both subtle finger inputs and dynamic hand gestures by installing the conventional wristband-based hand sensing system to the wristband coil. Moreover, the attachment of the multiple rings to both hands could provide uni-manual thumb-to-index input interface. For example, wearing two picoRing *joystick* to the left and right index fingers can enable wearable VR/AR game controller, almost similar to the standard VR/AR controllers.

9 CONCLUSION

This paper proposed picoRing, enabling a battery-free ring-based finger input device. With the combination of the sensitive coil, the sensitive impedance measurement circuit, and the sensitive peak detection, picoRing could pair a compact wristband coil with a tiny battery-free ring coil up to 13 cm away from the wristband despite the finger bending and metal near the wrist. picoRing also demonstrated that the ring coil could detect the basic subtle finger inputs including press, 1-D/2-D slide, or scroll, by using different passive switches. The development of the single ring coil supporting various finger inputs could be one of our main future work. We strongly believe the battery-free design of picoRing can be applied to other accessories such as earbuds, gloves, stylus, etc., and could promote the ubiquitous development of battery-free wearable input function into various accessories.

ACKNOWLEDGMENTS

REFERENCES

[1] Daniel Ashbrook, Patrick Baudisch, and Sean White. 2011. Nenya: Subtle and Eyes-Free Mobile Input with a Magnetically-Tracked Finger Ring. In *Proceedings of the SIGCHI Conference on Human Factors in Computing Systems* (Vancouver, BC, Canada) *(CHI '11)*. New York, NY, USA, 2043–2046. https://doi.org/10.1145/1978942.1979258

[2] Ravin Balakrishnan and I. Scott MacKenzie. 1997. Performance Differences in the Fingers, Wrist, and Forearm in Computer Input Control. In *Proceedings of the ACM SIGCHI Conference on Human Factors in Computing Systems* (Atlanta, Georgia, USA) *(CHI '97)*. Association for Computing Machinery, New York, NY, USA, 303–310. https://doi.org/10.1145/258549.258764

[3] Roger Boldu, Alexandru Dancu, Denys J.C. Matthies, Thisum Buddhika, Shamane Siriwardhana, and Suranga Nanayakkara. 2018. FingerReader2.0: Designing and Evaluating a Wearable Finger-Worn Camera to Assist People with Visual Impairments While Shopping. *Proc. ACM Interact. Mob. Wearable Ubiquitous Technol.* 2, 3, Article 94 (sep 2018), 19 pages. https://doi.org/10.1145/3264904

[4] Edwin Chan, Teddy Seyed, Wolfgang Stuerzlinger, Xing-Dong Yang, and Frank Maurer. 2016. User Elicitation on Single-Hand Microgestures. In *Proceedings of the 2016 CHI Conference on Human Factors in Computing Systems* (San Jose, California, USA) *(CHI '16)*. Association for Computing Machinery, New York, NY, USA, 3403–3414. https://doi.org/10.1145/2858036.2858589

[5] Liwei Chan, Rong-Hao Liang, Ming-Chang Tsai, Kai-Yin Cheng, Chao-Huai Su, Mike Y. Chen, Wen-Huang Cheng, and Bing-Yu Chen. 2013. FingerPad: Private and Subtle Interaction Using Fingertips. In *Proceedings of the 26th Annual ACM Symposium on User Interface Software and Technology* (St. Andrews, Scotland, United Kingdom) *(UIST '13)*. Association for Computing Machinery, New York, NY, USA, 255–260. https://doi.org/10.1145/2501988.2502016

[6] Ke-Yu Chen, Shwetak N. Patel, and Sean Keller. 2016. Finexus: Tracking Precise Motions of Multiple Fingertips Using Magnetic Sensing. In *Proceedings of the 2016 CHI Conference on Human Factors in Computing Systems*. New York, NY, USA, 1504–1514. https://doi.org/10.1145/2858036.2858125

[7] Taizhou Chen, Tianpei Li, Xingyu Yang, and Kening Zhu. 2023. EFRing: Enabling Thumb-to-Index-Finger Microgesture Interaction through Electric Field Sensing Using Single Smart Ring. *Proc. ACM Interact. Mob. Wearable Ubiquitous Technol.* 6, 4, Article 161 (jan 2023), 31 pages. https://doi.org/10.1145/3569478

[8] Bruce Cook and I.J Lowe. 1982. A large-inductance, high-frequency, high-Q, series-tuned coil for NMR. *Journal of Magnetic Resonance (1969)* 49, 2 (9 1982), 346–349. https://doi.org/10.1016/0022-2364(82)90200-1

[9] Artem Dementyev and Joseph A. Paradiso. 2014. WristFlex: Low-Power Gesture Input with Wrist-Worn Pressure Sensors. In *Proceedings of the 27th Annual ACM Symposium on User Interface Software and Technology* (Honolulu, Hawaii, USA) *(UIST '14)*. Association for Computing Machinery, New York, NY, USA, 161–166. https://doi.org/10.1145/2642918.2647396

[10] Masaaki Fukumoto and Yoshinobu Tonomura. 1997. "Body coupled FingerRing": Wireless Wearable Keyboard. In *Proceedings of the SIGCHI conference on Human factors in computing systems - CHI '97*. New York, NY, USA, 147–154. https://doi.org/10.1145/258549.258636

[11] Jun Gong, Yang Zhang, Xia Zhou, and Xing-Dong Yang. 2017. Pyro: Thumb-Tip Gesture Recognition Using Pyroelectric Infrared Sensing. In *Proceedings of the 30th Annual ACM Symposium on User Interface Software and Technology - UIST '17*. New York, NY, USA, 553–563. https://doi.org/10.1145/3126594.3126615

[12] Tovi Grossman, Xiang Anthony Chen, and George Fitzmaurice. 2015. Typing on Glasses: Adapting Text Entry to Smart Eyewear. In *Proceedings of the 17th International Conference on Human-Computer Interaction with Mobile Devices and Services* (Copenhagen, Denmark) *(MobileHCI '15)*. Association for Computing Machinery, New York, NY, USA, 144–152. https://doi.org/10.1145/2785830.2785867

[13] Jan Gugenheimer, David Dobbelstein, Christian Winkler, Gabriel Haas, and Enrico Rukzio. 2016. FaceTouch: Enabling Touch Interaction in Display Fixed UIs for Mobile Virtual Reality. In *Proceedings of the 29th Annual Symposium on User Interface Software and Technology* (Tokyo, Japan) *(UIST '16)*. Association for Computing Machinery, New York, NY, USA, 49–60. https://doi.org/10.1145/2984511.2984576

[14] Aakar Gupta, Cheng Ji, Hui-Shyong Yeo, Aaron Quigley, and Daniel Vogel. 2019. RotoSwype: Word-Gesture Typing Using a Ring. In *Proceedings of the 2019 CHI Conference on Human Factors in Computing Systems* (Glasgow, Scotland Uk) *(CHI '19)*. Association for Computing Machinery, New York, NY, USA, 1–12. https://doi.org/10.1145/3290605.3300244

[15] Jiawei Huang, Ryo Sugawara, Kinfung Chu, Taku Komura, and Yoshifumi Kitamura. 2022. Reconstruction of Dexterous 3D Motion Data From a Flexible Magnetic Sensor With Deep Learning and Structure-Aware Filtering. *IEEE Transactions on Visualization and Computer Graphics* 28, 6 (2022), 2400–2414. https://doi.org/10.1109/TVCG.2020.3031632

[16] Shuo Jiang, Peiqi Kang, Xinyu Song, Benny P.L. Lo, and Peter B. Shull. 2022. Emerging Wearable Interfaces and Algorithms for Hand Gesture Recognition: A Survey. *IEEE Reviews in Biomedical Engineering* 15 (2022), 85–102. https://doi.org/10.1109/RBME.2021.3078190

[17] Wolf Kienzle and Ken Hinckley. 2014. LightRing: Always-Available 2D Input on Any Surface. In *Proceedings of the 27th Annual ACM Symposium on User Interface Software and Technology* (Honolulu, Hawaii, USA) *(UIST '14)*. New York, NY, USA, 157–160. https://doi.org/10.1145/2642918.2647376

[18] Wolf Kienzle, Eric Whitmire, Chris Rittaler, and Hrvoje Benko. 2021. ElectroRing: Subtle Pinch and Touch Detection with a Ring *(CHI '21)*. New York, NY, USA, Article 3, 12 pages. https://doi.org/10.1145/3411764.3445094

[19] Daehwa Kim and Chris Harrison. 2022. EtherPose: Continuous Hand Pose Tracking with Wrist-Worn Antenna Impedance Characteristic Sensing. In *Proceedings of the 35th Annual ACM Symposium on User Interface Software and Technology* (Bend, OR, USA) *(UIST '22)*. New York, NY, USA, Article 58, 12 pages. https://doi.org/10.1145/3526113.3545665

[20] Gierad Laput, Robert Xiao, and Chris Harrison. 2016. ViBand: High-Fidelity Bio-Acoustic Sensing Using Commodity Smartwatch Accelerometers. In *Proceedings of the 29th Annual Symposium on User Interface Software and Technology* (Tokyo, Japan) *(UIST '16)*. Association for Computing Machinery, New York, NY, USA, 321–333. https://doi.org/10.1145/2984511.2984582

[21] Chen Liang, Chun Yu, Yue Qin, Yuntao Wang, and Yuanchun Shi. 2021. DualRing: Enabling Subtle and Expressive Hand Interaction with Dual IMU Rings. *Proc. ACM Interact. Mob. Wearable Ubiquitous Technol.* 5, 3, Article 115 (sep 2021), 27 pages. https://doi.org/10.1145/3478114

[22] Rongzhou Lin, Han-Joon Kim, Sippanat Achavananthadith, Selman A. Kurt, Shawn C. C. Tan, Haicheng Yao, Benjamin C. K. Tee, Jason K. W. Lee, and John S. Ho. 2020. Wireless battery-free body sensor networks using near-field-enabled clothing. *Nature Communications* 11, 1 (2020), 444. https://doi.org/10.1038/s41467-020-14311-2

[23] C.G.M. Meskers, H.M. Vermeulen, J.H. de Groot, F.C.T. van der Helm, and P.M. Rozing. 1998. 3D shoulder position measurements using a six-degree-of-freedom electromagnetic tracking device. *Clinical Biomechanics* 13, 4 (1998), 280–292. https://doi.org/10.1016/S0268-0033(98)00095-3

[24] Saman Naderiparizi, Mehrdad Hessar, Vamsi Talla, Shyamnath Gollakota, and Joshua R Smith. 2018. Towards Battery-Free HD Video Streaming. In *15th USENIX Symposium on Networked Systems Design and Implementation (NSDI 18)*. USENIX Association, Renton, WA, 233–247.

[25] Shahriar Nirjon, Jeremy Gummeson, Dan Gelb, and Kyu-Han Kim. 2015. TypingRing: A Wearable Ring Platform for Text Input. In *Proceedings of the 13th Annual International Conference on Mobile Systems, Applications, and Services* (Florence, Italy) *(MobiSys '15)*. New York, NY, USA, 227–239. https://doi.org/10.1145/2742647.2742665

[26] Farshid Salemi Parizi, Eric Whitmire, and Shwetak Patel. 2019. AuraRing: Precise Electromagnetic Finger Tracking. *Proceedings of the ACM on Interactive, Mobile, Wearable and Ubiquitous Technologies* 3, 4 (12 2019), 1–28. https://doi.org/10.1145/3369831

[27] Frederick H. Raab, Ernest B. Blood, Terry O. Steiner, and Herbert R. Jones. 1979. Magnetic Position and Orientation Tracking System. *IEEE Trans. Aerospace Electron. Systems* AES-15, 5 (1979), 709–718. https://doi.org/10.1109/TAES.1979.308860

[28] Jun Rekimoto. 2001. GestureWrist and GesturePad: unobtrusive wearable interaction devices. In *Proceedings Fifth International Symposium on Wearable Computers*.

[29] Gabriel Reyes, Jason Wu, Nikita Juneja, Maxim Goldshtein, W. Keith Edwards, Gregory D. Abowd, and Thad Starner. 2018. SynchroWatch: One-Handed Synchronous Smartwatch Gestures Using Correlation and Magnetic Sensing. 1, 4, Article 158 (jan 2018), 26 pages. https://doi.org/10.1145/3161162

[30] T. Scott Saponas, Desney S. Tan, Dan Morris, Ravin Balakrishnan, Jim Turner, and James A. Landay. 2009. Enabling Always-Available Input with Muscle-Computer Interfaces. In *Proceedings of the 22nd Annual ACM Symposium on User Interface Software and Technology* (Victoria, BC, Canada) *(UIST '09)*. Association for Computing Machinery, New York, NY, USA, 167–176. https://doi.org/10.1145/1622176.1622208

[31] Ryo Takahashi, Masaaki Fukumoto, Changyo Han, Takuya Sasatani, Yoshiaki Narusue, and Yoshihiro Kawahara. 2020. TelemetRing: A Batteryless and Wireless Ring-Shaped Keyboard Using Passive Inductive Telemetry. In *Proceedings of the 33rd Annual ACM Symposium on User Interface Software and Technology* (Virtual Event, USA) *(UIST '20)*. New York, NY, USA, 1161–1168. https://doi.org/10.1145/3379337.3415873

[32] Ryo Takahashi, Wakako Yukita, Takuya Sasatani, Tomoyuki Yokota, Takao Someya, and Yoshihiro Kawahara. 2022. Twin Meander Coil: Sensitive Readout of Battery-Free On-Body Wireless Sensors Using Body-Scale Meander Coils. *Proc. ACM Interact. Mob. Wearable Ubiquitous Technol.* 5, 4, Article 179 (dec 2022), 21 pages. https://doi.org/10.1145/3494996

[33] Ryo Takahashi, Wakako Yukita, Tomoyuki Yokota, Takao Someya, and Yoshihiro Kawahara. 2022. Meander Coil++: A Body-Scale Wireless Power Transmission Using Safe-to-Body and Energy-Efficient Transmitter Coil. In *Proceedings of the 2022 CHI Conference on Human Factors in Computing Systems* (New Orleans, LA, USA) *(CHI '22)*. New York, NY, USA, Article 390, 12 pages. https://doi.org/10.1145/3491102.3502119

[34] Andrew Vardy, John Robinson, and Li-Te Cheng. 1999. The WristCam as input device. In *Digest of Papers. Third International Symposium on Wearable Computers*. 199–202. https://doi.org/10.1109/ISWC.1999.806928

[35] Radu-Daniel Vatavu. 2023. IFAD Gestures: Understanding Users' Gesture Input Performance with Index-Finger Augmentation Devices. In *Proceedings of the 2023 CHI Conference on Human Factors in Computing Systems* (Hamburg, Germany) *(CHI '23)*. Association for Computing Machinery, New York, NY, USA, Article 576, 17 pages. https://doi.org/10.1145/3544548.3580928

[36] Anandghan Waghmare, Roger Boldu, Eric Whitmire, and Wolf Kienzle. 2023. OptiRing: Low-Resolution Optical Sensing for Subtle Thumb-to-Index Micro-Interactions. In *Proceedings of the 2023 ACM Symposium on Spatial User Interaction* (Sydney, NSW, Australia) *(SUI '23)*. Association for Computing Machinery, New York, NY, USA, Article 8, 13 pages. https://doi.org/10.1145/3607822.3614538

[37] Erwin Wu, Ye Yuan, Hui-Shyong Yeo, Aaron Quigley, Hideki Koike, and Kris M. Kitani. 2020. Back-Hand-Pose: 3D Hand Pose Estimation for a Wrist-Worn Camera via Dorsum Deformation Network. In *Proceedings of the 33rd Annual ACM Symposium on User Interface Software and Technology* (Virtual Event, USA) *(UIST '20)*. Association for Computing Machinery, New York, NY, USA, 1147–1160. https://doi.org/10.1145/3379337.3415897

[38] Chenhan Xu, Bing Zhou, Gurunandan Krishnan, and Shree Nayar. 2023. AO-Finger: Hands-Free Fine-Grained Finger Gesture Recognition via Acoustic-Optic Sensor Fusing. In *Proceedings of the 2023 CHI Conference on Human Factors in Computing Systems* (Hamburg, Germany) *(CHI '23)*. Association for Computing Machinery, New York, NY, USA, Article 306, 14 pages. https://doi.org/10.1145/3544548.3581264

[39] Xuhai Xu, Jun Gong, Carolina Brum, Lilian Liang, Bongsoo Suh, Shivam Kumar Gupta, Yash Agarwal, Laurence Lindsey, Runchang Kang, Behrooz Shahsavari, Tu Nguyen, Heriberto Nieto, Scott E Hudson, Charlie Maalouf, Jax Seyed Mousavi, and Gierad Laput. 2022. Enabling Hand Gesture Customization on Wrist-Worn Devices. In *Proceedings of the 2022 CHI Conference on Human Factors in Computing Systems* (New Orleans, LA, USA) *(CHI '22)*. Association for Computing Machinery, New York, NY, USA, Article 496, 19 pages. https://doi.org/10.1145/3491102.3501904

[40] Shumin Zhai, Paul Milgram, and William Buxton. 1996. The Influence of Muscle Groups on Performance of Multiple Degree-of-Freedom Input. In *Proceedings of the SIGCHI Conference on Human Factors in Computing Systems* (Vancouver, British Columbia, Canada) *(CHI '96)*. Association for Computing Machinery, New York, NY, USA, 308–315. https://doi.org/10.1145/238386.238534

[41] Yang Zhang, Robert Xiao, and Chris Harrison. 2016. Advancing Hand Gesture Recognition with High Resolution Electrical Impedance Tomography. In *Proceedings of the 29th Annual Symposium on User Interface Software and Technology* (Tokyo, Japan) *(UIST '16)*. Association for Computing Machinery, New York, NY, USA, 843–850. https://doi.org/10.1145/2984511.2984574